Systemic and cerebral hemodynamics in response to cardiovascular challenges : the heart-brain connection

Verbree, J.

CHAPTER 7

Transcranial Doppler determined middle cerebral artery blood flow velocity does not match MRI global or regional cerebral tissue perfusion during handgrip exercise

Jasper Verbree*
Anne-Sophie G.T. Bronzwaer*
Mark A. van Buchem
M.A.A. van Walderveen
Mat J.A.P. Daemen
Johannes J. van Lieshout
Matthias J.P. van Osch
* These authors contributed equally

Submitted

ABSTRACT

Changes in Transcranial Doppler (TCD) determined cerebral blood flow velocity (CBFv) are regularly considered to reflect (proportional) changes in cerebral blood flow (CBF), for instance during exercise. However, neuroimaging studies indicated a localized and smaller CBF increase compared to the CBFv changes. The aim of this study was to validate this interpretation by comparing the TCD measured velocity response to rhythmic handgrip exercise with the regional CBF response assessed with Arterial Spin Labeling (ASL) MRI. Thirty-eight healthy subjects completed an exercise protocol of three times 5 minutes of rhythmic handgrip. In the first session, the cerebral hemodynamic response to handgrip was assessed by TCD and during the second session by ASL-MRI. No difference in heart-rate response was observed between TCD and MRI sessions and $PetCO_2$ remained unchanged. During handgrip CBFv increased by 10.7±11.7%, whereas no change in CBF in the MCA flow territory was detected by ASL MRI (-1.2±10.4%, $p = 0.18$); regional CBF increased by 7.8±10.1% in the precentral region. Therefore, changes in CBFv do not reflect changes in the underlying flow territory CBF and/or regional CBF. These findings call into question the nature or the disparity between large artery flow velocity and brain tissue flow in response to rhythmic handgrip.

Keywords

Arterial spin labeling; cerebral blood flow; rhythmic handgrip; MRI; transcranial Doppler

INTRODUCTION

During exercise the brain is activated [1-3], and locally enhanced neuronal activity and energy demand [4,5] increase cerebral blood flow (CBF) in specific areas of the brain [6-8]. Transcranial Doppler (TCD) determined cerebral blood flow velocity (CBFv) in large brain-feeding arteries is commonly used as proxy for CBF [9]. During dynamic exercise with large muscle groups (e.g. cycling exercise) CBFv varies in parallel with ^{133}Xe clearance measures of CBF [10,11], with Fick-determined CBF [12], and with internal [13,14] and common carotid artery flow [15]. In contrast, high spatial resolution neuroimaging studies evidenced that upon static handgrip [16,17], rhythmic handgrip [18] and cycling [19-21] increases CBF in specific cortical regions only. This increase in regional CBF (rCBF) occurs in only a small sub-region of the flow territory of the artery in which TCD measures the velocity. The much smaller volume sub-region involved in neuronal activation during exercise suggests that the change in flow territory CBF (ftCBF) is much smaller than the CBFv increase in large brain arteries.

For example, the CBF change upon mild to moderate exercise of 10–15% [17-19] is limited to the motor cortex, which comprises only 3% of the entire MCA flow territory [22]. Combining these numbers suggests that the ftCBF increases by 0.3–0.5%. However, TCD observations during dynamic handgrip exercise showed that MCAv increases by 8–19% [23-31]. Depending on the location of measurement either the ftCBF increases negligible (<1%) using spatially resolved CBF or substantial (~10%) when assessed with CBFv. We therefore question whether CBFv is a valid proxy for CBF during small muscle group exercise. This study addressed whether the increase in CBFv during exercise matches the CBF-change within the corresponding flow territory or within the activated brain region. To that purpose the study compared CBFv and MRI-determined CBF in healthy subjects during dynamic handgrip exercise.

MATERIALS AND METHODS

Subjects

57 non-smoking subjects were included in the study. The study was performed in accordance with the Helsinki protocol, as approved by the institutional Medical Ethics Committee of the Academic Medical Center in Amsterdam. Written informed consent was obtained from all participants prior to the medical screening. All subjects underwent a medical screening on a separate day prior to the experiment consisting of a medical interview, fasting blood sampling (including plasma hemoglobin, hematocrit, HbA1C, creatinine, glucose, total-, HDL- and LDL-cholesterol), urine-testing and a 12-lead electrocardiogram (ECG). Subjects were excluded from participation in case of cardiovascular disease, hypertension, diabetes mellitus and/or neurological disease, use of vasoactive medication, abnormal lab-results, abnormal ECG and/or smoking or having smoked <10 years ago. Subjects were instructed to abstain from alcoholic and caffeinated beverages for at least 4 hours prior to the experiment.

Sessions

All subjects performed the same exercise protocol in two measurement sessions in fixed order, separated by 8±4 days. During the first (TCD) session, continuous CBFv, non-invasive blood pressure (BP), heart rate (HR) and end-tidal CO_2 ($PetCO_2$) responses to small muscle group exercise (dynamic handgrip) were determined. In the second (MRI) session, the spatial distribution of CBF during dynamic handgrip was assessed.

Exercise protocol

Three bouts of 5-minute rhythmic handgrip exercise were alternated with 5 minutes of rest. Prior to the measurements, maximum voluntary contraction (MVC) was measured using an MRI compatible handgrip device (Gripforce 500N, Curdes design, Philadelphia PA, USA). The highest value of three measurements was set as MVC for the duration of the experiment. To achieve and maintain a steady state hemodynamic response to exercise, one minute of rhythmic handgripping at 80% MVC was followed by 60% MVC for 4 minutes. Visual feedback of the exercise rhythm (2 seconds contraction, 2 seconds rest) and the force applied by the volunteer were displayed either on a laptop (TCD session) or onto a screen in the MRI scanner.

TCD session

Subjects were in the supine position with the head supported by a pillow. Changes in CBFv were monitored in the proximal segment of the MCA by means of transcranial Doppler ultrasonography (DWL Multidop X4, Sipplingen, Germany) using a pulsed 2 MHz TCD probe at a depth of 45–55 mm [9]. The MCA contralateral to the handgripping hand was insonated through the temporal-window above the zygomatic arch at a depth of 40–60 mm. After signal optimization [24], the probe was immobilized by a head-band. Continuous BP and heart rate (HR) was measured non-invasively by finger plethysmography with an inflatable cuff placed around the middle finger of the non-dominant hand (Nexfin, Edwards Lifesciences BMEYE, the Netherlands). End-tidal CO_2 ($PetCO_2$) was continuously monitored by a nasal cannula connected to a capnograph (Datex Normocap 200, Helsinki, Finland).

MRI session

Changes in CBF were measured with a 3 Tesla Philips Achieva TX MR system (Philips, Best, The Netherlands), using a commercial 32-channel head coil. Subjects were instructed not to move their head and additional foam padding next to the head minimized motion.

A detailed listing of scanning parameters is given in Table 7.1. The MRI protocol included a whole-brain T_1-weighted anatomical scan for anatomical depiction and gray matter segmentation, FLAIR of the brain and 3D Phase-Contrast angiography of the brain-feeding arteries. An experienced neuroradiologist (MvW) evaluated these images for structural abnormalities and the presence of carotid stenosis.

Table 7.1 | Summary of MRI scan parameters for anatomical and CBF measurements.

	Anatomical T1-weighted	**Dual Echo pCASL**	**M0**	**Phase Contrast angiogram**	**FLAIR**
Planning orientation	Transverse	Transverse	Transverse	Coronal, covering neck arteries	Transverse
Scan Technique	3D Fast Field Echo	Multi Slice Gradient Echo	Multi Slice Gradient Echo	3D Fast Field Echo	Multi slice, Inversion Recovery
Acceleration type	TFE factor 179, SENSE 1.8 RL	SENSE factor 3, EPI factor 25	SENSE factor 3, EPI factor 25	SENSE 2 RL 3 AP, Halfscan 0.85	SENS 1.75 RL, TSE factor 41
Repetition time/echo time	9.8 / 4.6 ms	4500 ms / 11 & 28.5 ms	2000 ms / 11 & 28.5 ms	10 / 6.2 ms	11000 / 120 ms
Flip / Refocusing angle	8° / –	90° / –	90° / –	10° / –	– / 120°
Field of view	224 x 176 x 168 mm^3	220 x 220 x 102 mm^3	220 x 220 x 102 mm^3	230 x 170 x 180 mm^3	230 x 184 x 119 mm^3
Acquisition voxel size	1.19 / 1.21 / 1.20 mm^3	2.75 x 2.75 x 6 mm^3	2.75 x 2.75 x 6 mm^3	0.99 / 1.00 / 2.00	0.96 / 1.33 / 4.00 mm^3
Acquisition matrix	188 x 146	72 x 69	72 x 69	232 x 170	240 x 138
Scan duration	2:47 min	30 min (400 dynamics)	22 sec (10 averages)	1:45 min	01:39 min
Labeling / PLD duration	–	1800 ms / 1800 ms	no labeling	–	–
Additional parameters	Inversion delay 935 ms	BGS pulses 1850 & 3175 ms	No BGS pulses	VENC 80 cm/s (uniform)	Inversion time 2800 ms
TFE dur. shot / acq	1938 / 1757 ms	–	–	–	–

TFE: Turbo Field Techo; BGS Background suppression; VENC: velocity encoding; SENSE: parallel imaging technique

CBF was assessed continuously during the exercise protocol using pseudo-continuous arterial spin labeling (pCASL) [32] with similar settings as in Ghariq et al. [33]. The ASL imaging volume was positioned to cover the cerebrum, and the labeling plane was planned perpendicular to the internal carotid arteries at the level of the basilar artery. Two background suppression pulses were applied after labeling to improve signal to noise ratio [34,33]. Finally, a separate M_0 scan was acquired to enable quantification of CBF (TR_{M0} = 2000ms).

Heart rate was derived from the finger pulse oximetry plethysmogram, either by the build-in scanner unit, or by a patient monitoring device (Magnitude, In-Vivo, Philadelphia, California). $PetCO_2$ was sampled with a nasal cannula connected to a capnograph located outside the scanner (Capnomac Ultima, Datex, Helsinki, Finland), or the patient monitoring device. In a subset of subjects, blood pressure was monitored during resting conditions using the patient monitoring device. All signals were synchronized to the acquisition of the ASL scan.

MRI post-processing

The ASL images were preprocessed to obtain CBF values according to the procedures laid out in the consensus paper [32]. All preprocessing steps were done within the Matlab 2016a coding environment (Mathworks, Natick, Massachusetts, U.S.A) using SPM12 (http://www.fil.ion.ucl.ac.uk/spm/), ASLtbx [35], and AAL [36] toolboxes. The anatomical T1-weighted scan was segmented into CSF, white- and gray matter probability maps. Motion correction of the ASL series was performed using ASLtbx, taking into account the signal intensity gradient introduced by background suppression [33]. The motion corrected ASL image volumes were pairwise subtracted (control – label) and converted to units of flow according to the consensus model [32]:

$$CBF = \frac{6000 \cdot e^{\frac{PLD}{T_{1,blood}}}}{2 \cdot \alpha \cdot T_{1,blood} \cdot (1 - e^{\frac{lbldur}{T_{1,blood}}})} \cdot \frac{SI_{control} - SI_{label}}{M_0}$$

where SI represents the spatially varying ASL signal intensity during control and label conditions. Reported values in literature for $T_{1,blood}$ (1665 ms) and labeling efficiency (α = 0.85) were assumed. The PLD was corrected for the time-difference of the readout of the slices, starting at 1800 ms for the first slice increasing by 48 ms for subsequent slices. The M_0-image was calculated from the M_0 scan by smoothing with a 5 mm FWHM 3D kernel, thresholded to limit the scan to brain tissue, and was corrected for finite TR with $(1-\exp(-TR_{M0}/T_{1,gm}))^{-1}$, with $T_{1,gm}$ assumed to be 1260 ms. The temporal mean of the CBF-series was co-registered to the gray matter probability map (SPM, Intensity Normalization metric).

MRI regions of interest

Regions of interest (ROIs) were defined to calculate the rCBF at multiple locations in the brain. For each subject, the single-subject AAL atlas [36] (Figure 7.1) was non-linearly deformed (warped) to the T_1-weighted anatomical scan using the inverse transform obtained during the segmentation

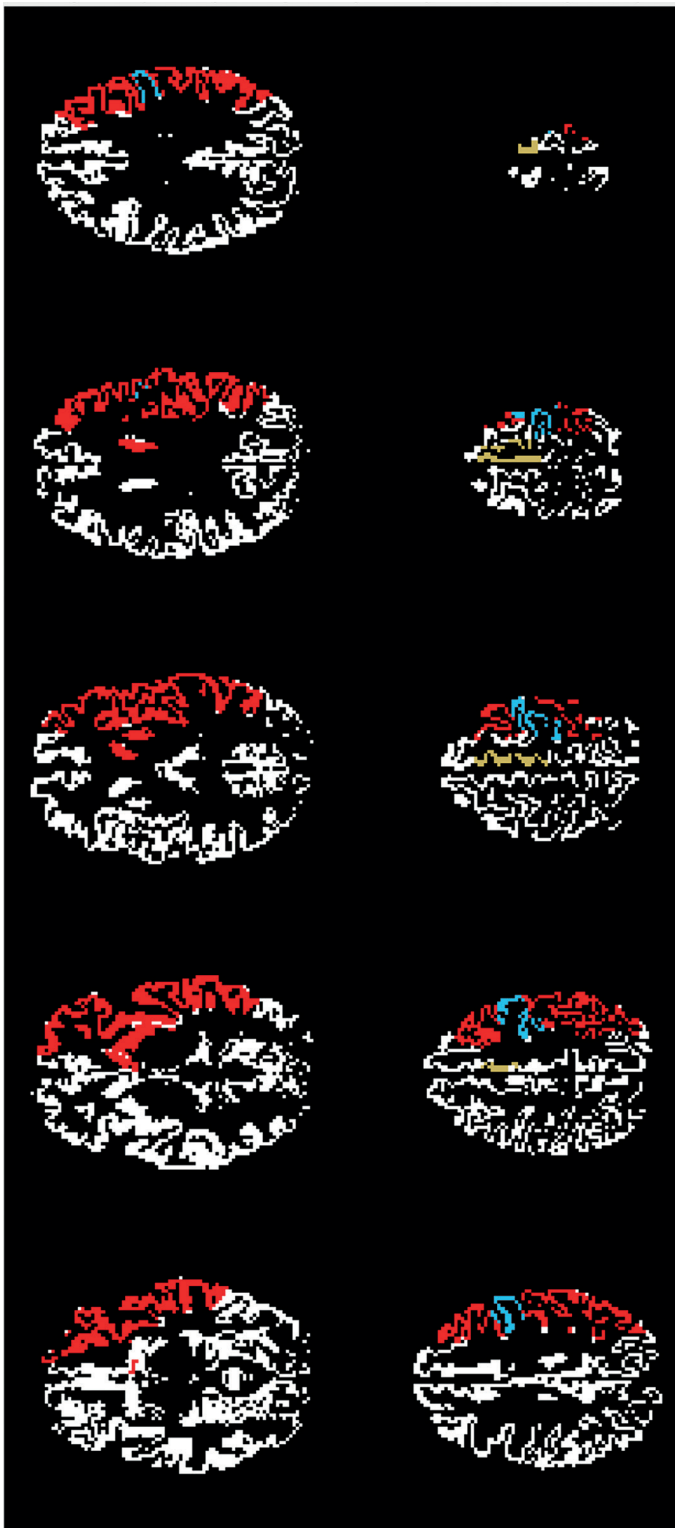

Figure 7.1 | Illustration of the grey matter mask of a representative subject. Regions of interest are indicated with color, showing MCA (red), precentral cortex (blue) and supplementary motor area (yellow).

step. The resulting subject-specific atlas was visually checked by overlaying the ROIs on the anatomical scan. All ROIs were masked by the gray matter probability map (threshold >0.9). Relative volumes of the ROI were calculated individually (in native space) by counting the number of voxels and converting to mL. ROIs were subsequently transferred to the CBF-maps, which were co-registered to the T_1-weighted anatomical scan during the MRI post-processing steps (see above). Lower regions in the brain, e.g. vermis, brainstem and cerebellum were excluded from analysis due to a limited field-of-view of the ASL imaging module in the feet-head direction. The remaining ROIs of the AAL atlas were grouped in ACA, MCA and PCA flow territories [37]. The extent and overlap of flow territories can differ substantially between individuals, therefore next to the nominal MCA flow territory, a conservative and a liberal estimate of the MCA-territory were defined based on a surgical-anatomical atlas [37]. Specific regional CBF changes were investigated in the precentral and supplementary motor area (SMA) ROI as these regionals are generally associated with motor function. The MRI data of left handed subjects (n = 4) were mirrored before further analysis. To quantify the effect of visual feedback, a visual cortex ROI was defined by combining the calcarine and superior-, middle- and inferior occipital cortex.

Statistics and data analysis

Data from the TCD and MRI sessions were visually inspected and images with artifacts were excluded from analysis. The signals of BP, the envelope curve of the transcranial Doppler spectrum from the MCA and $PETCO_2$ were A/D converted at 200 Hz and stored. Mean arterial pressure (MAP), HR and the mean CBFv were calculated per heart-beat. Data were averaged over the three runs and the averaged values over the last 3 minutes of each episode of both rest or handgrip were used as steady-state values. Statistical analysis was performed using the Statistics toolbox of Matlab (v2016a). Differences within and between sessions (TCD and MRI) were inferred using paired *t*-test and ANOVA after confirming a normal distribution of the data using the Lilliefors test). The relation between the change in CBFv and CBF in predefined ROI's was investigated by regression analysis. Levene's test was used to assess the assumption of equal variances and normality of the residuals was inspected.

RESULTS

Subjects

Seven subjects were excluded based on the results of medical screening, and one subject declined participation after the screening process. Technical issues resulted in incomplete data in 10 subjects, and one additional subject had a structural abnormality on the MRI scans. The final analysis was performed on the data of the remaining 38 subjects (13 female) with a median age of 55 years (range: 19–79).

Systemic response

Resting values and responses to handgrip for both sessions are summarized in Table 7.2. Resting HR, $PetCO_2$ and MAP were similar for the TCD and MRI sessions. During handgrip, HR increased similarly in TCD (10±5%, p<0.01) and MRI (9±7%, p<0.01) sessions (between sessions p = 0.23). No change in $PetCO_2$ was detected in either session (p = 0.10 and p = 0.08 for TCD and MRI respectively). MAP increased in the TCD session by 10±5% (p<0.01) during handgrip (MAP response was not assessed during the MRI session).

Table 7.2 | Systemic response to rhythmic handgrip in the TCD and MRI sessions.

		TCD		MRI	
		Rest	**Handgrip (%Delta)**	**Rest**	**Handgrip (%Delta)**
HR	(bpm)	59±7	10±5%**	60±8†	9±7%**
$PetCO_2$	(mmHg)	39.9±3.5	1.5±4.8%	40.3±4.5†	-0.9±3.6%§
MAP	(mmHg)	9 ±9	10±5%**	94±11†	–
CBFv / CBFmca	(cm/s / ml/100g/min)	60±14	11±12%**	46±10	-1±10%

HR: heart rate; MAP: mean arterial pressure; CBFv: cerebral blood flow velocity measured by TCD; CBFmca: CBF in the MCA flow territory measured by MRI. *) p<0.05, **) p<0.01 vs. Rest; †) p = n.s. vs. TCD Rest; §) p<0.05, §§) p<0.01 vs. %Delta TCD; Values are means±SD.

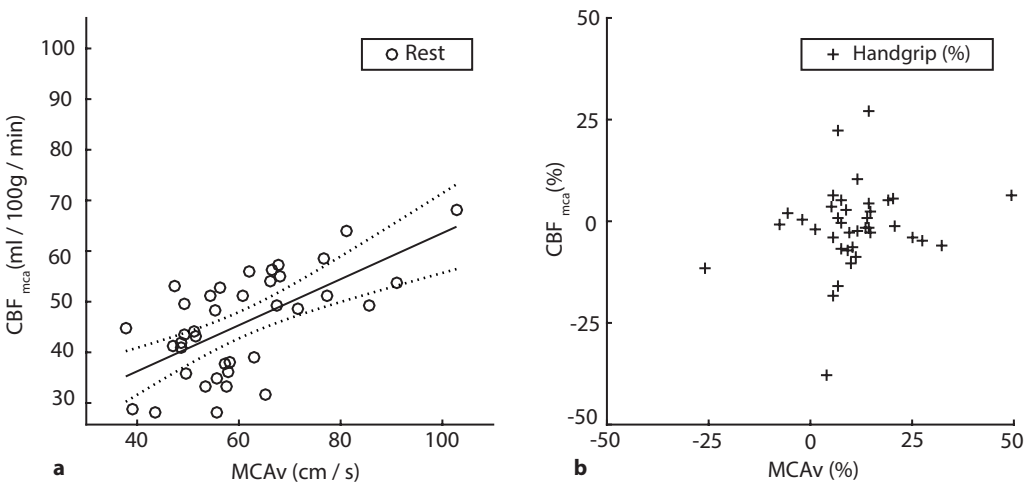

Figure 7.2 | Comparison of CBFv and CBF averaged over the MCA ROI (CBF_{mca}). **a**) Absolute values during rest with regression line CBFmca = 17.8 + 0.46·CBFv (p<0.001) (solid line) and 95% confidence interval (dotted line); **b**) relative response to handgrip.

Flow territory CBF versus CBFv

Both CBFv and ftCBF in the MCA flow territory ROI responses were measured in the hemisphere contralateral to the exercising hand (see Figure 7.2). During rhythmic handgrip, CBFv increased (11 ± 12%, p<0.01), while no change was found in ftCBF (-1±10%, p = 0.15). The absence of CBF change in the normal MCA flow territory definition was confirmed for both the conservative (-0.0±10%) as well as for the liberal definition (+0.1±10%) of the ROI. During rest CBFv was linearly related to ftCBF (p<0.001), with a non-zero offset (p<0.01), see Figure 7.2a.

Regional CBF versus CBFv

In Figure 7.3 the relative change rCBF in the precentral ROI is depicted against the change in CBFv. During handgrip exercise rCBF increased in the contralateral (8±10%; p<0.01), but not in the ipsilateral precentral ROI (6±18%; p = 0.12). The increase in CBFv was not correlated to the regional CBF increase in the precentral ROI (r = 0.16, p = 0.35).

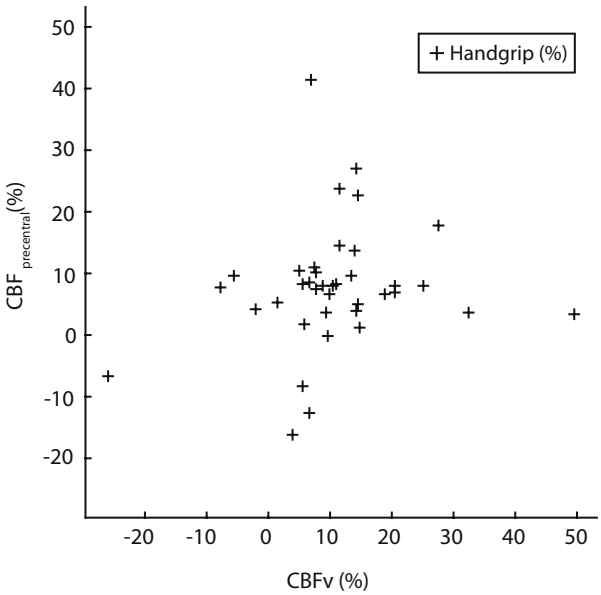

Figure 7.3 | Relative changes in CBFv and regional CBF (Precentral ROI) upon handgrip.

CBF in the contralateral SMA ROI increased (8±13%; p<0.01), but did not change in the ipsilateral ROI (±13%, p = 0.13). rCBF in the visual cortex ROI increased by 9±11% (p<0.01).

ROI Volume Estimates

Volume estimates of the MCA-, Precentral- and SMA ROIs are given in Table 7.3. The relative total volume of the precentral ROI was 10±1% of the total MCA ROI, whereas the precentral gray matter volume was 7±1% relative to the MCA gray matter volume.

Table 7.3 | Volume estimates of regions of interest.

	Total (mL)	GM (mL)	Relative Total (% MCA)	Relative GM (% MCA)
MCA flow territory	156±14	74±12		
Precentral	15±1	5±1	9.5±0.4%	7.0±0.7%
SMA	11±1	4±1	6.8±0.3%	5.7±0.4%

ROIs are contralateral to the side handgripping. GM: gray matter; SMA: supplementary motor area. Values are mean±SD.

DISCUSSION

This study addressed whether the increase in middle cerebral artery (MCA) blood flow velocity as measured by TCD during small muscle group exercise parallels CBF within the relevant area of the brain as measured by ASL-MRI. The main finding is that the CBFv increased by 11%, whereas no change could be detected in the corresponding flow territory CBF, although an 8% increase in rCBF was detected in the functional relevant brain regions. This finding calls into question the use of TCD velocity changes as a proxy for cerebral blood flow changes.

To illustrate this disparity, the locations of the CBFv and CBF measurements are graphically depicted in Figure 7.4. The observed increase in CBFv is well within the range (8–19%) previously reported by studies using rhythmic handgrip [23-31]. Traditionally, an increase in in CBFv is assumed to imply a ftCBF response. For example, a hypothetical rCBF increase of 110% in a tenth of the flow territory volume (see Table 7.3) is required to increase ftCBF by 11%, which is much larger than observed in this study or reported in MRI literature. Conversely, the observed 8% increase in rCBF would predict a 0.8% increase in ftCBF, which is clearly at odds with the observed increase in CBFv. Although in-between scenario's can be constructed, these black-and-white scenarios illustrate clearly the order of magnitude discrepancy between the measured CBFv and ftCBF.

Validity of ASL and TCD measurements

Assumptions of both TCD and ASL could attribute to the observed discrepancy. Particularly relevant are the assumptions that affect the percentage change as used the in the present study. Factors affecting only the quantitative scaling have been discussed elsewhere for TCD [38] and ASL-MRI [32].

In ASL-MRI, the labeling efficiency is dependent on the blood flow velocity of the arteries at the level of the labeling plane. Simulations showed that the efficiency decreases only by ~1% when velocity is increased by 20% [39,40], therefore it can be assumed that reduced labeling efficiency contributes little to the observed discrepancy. During exercise, faster blood flow shortens the transport time of the labeled blood to the tissue. Theoretically this could lead to an overestimation of the CBF-increase (more labeled blood arrives in the ROI), but could also lead

to an underestimation of the CBF response due to faster decay of the label in the tissue (label stays a shorter time in blood, whereas the T_1 of tissue is smaller than T_1 of blood). Finally, during exercise the T_2^* of the label might be prolonged due to the higher levels of blood oxygenation (BOLD-effect), leading again to an overestimation of the CBF-increase [41]. Therefore, it is difficult to provide a clear explanation why ASL-MRI would severely underestimate the mean CBF increase over the MCA-flow territory.

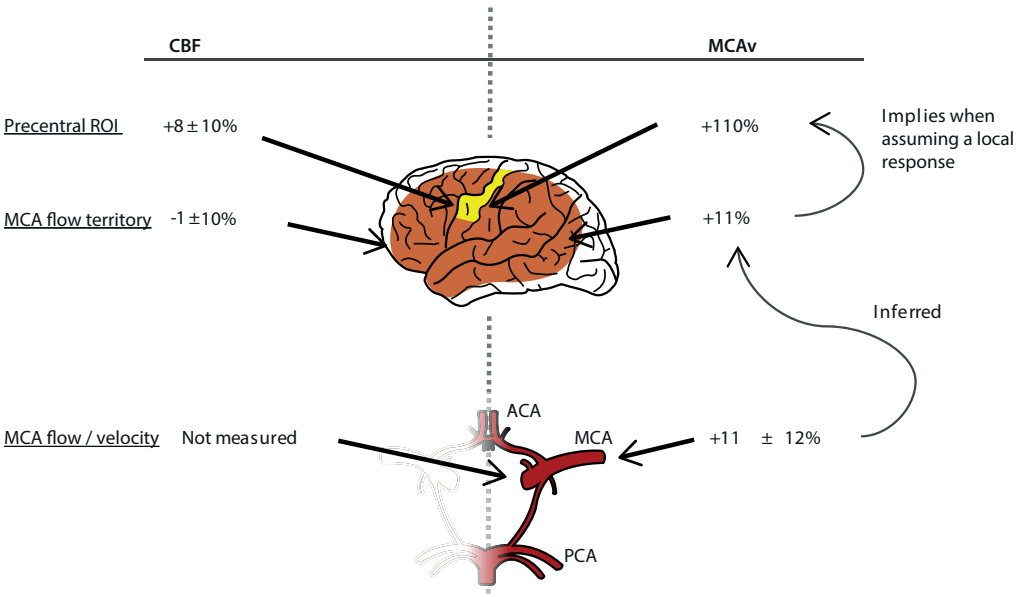

Figure 7.4 | Schematic representation of the location of the regional CBF and CBFv changes observed in the present study. Note that the CBF also increased outside the indicated areas: in particular, the supplementary motor area and visual cortex which are both not supplied by the MCA. Illustrations adapted from Wikimedia under the creative commons license.

An important assumption in TCD is the constancy of the MCA diameter. A decrease in MCA cross-sectional area would inverse-proportionally affect the flow, at constant velocity. In a previous study, we assessed the MCA cross-sectional area response during rhythmic handgrip exercise using high resolution MRI [42]. In that study, the exact same handgrip protocol was used as in the present study, although in a different study population (age range 20–59 years). On average a 2% decrease in cross-sectional area was observed. This difference is small and could maximally explain a fifth of the 11% CBFv increase observed in the present study. Therefore, the minimal change in MCA diameter during handgrip exercise is not the sole contributor to the discrepancy.

In transcranial Doppler ultrasonography, the reported change in CBFv is usually based on the average maximum velocity derived from TCD spectrum of multiple heart beats [9,38]. The maximum velocity is used as a proxy for the cross-sectional average velocity, which physically

defines flow. The relation between the maximum and cross-sectional velocity can be complex in the short and curved MCA (M1 segment), but is assumed stable when comparing beat-to-beat averages. Changes in the flow profile can offset this relation and maximum velocity potentially underestimates the changes in average cross-sectional velocity. However, CBFv matches the flow increase in the internal carotid artery during loaded cycling [43], rendering an important offset between maximum- and cross-sectional velocity unlikely.

In summary, both ASL and TCD both involve assumptions that could potentially under- or overestimate the change in cerebral perfusion upon exercise, but reasonable estimation of the order of magnitude of such errors limit these to a few percentage points. Hence these do not satisfactory explain the order of magnitude difference between the observed CBFv and CBF changes. Therefore, without clear evidence of the invalidity of either of the two modalities, other explanations need to be considered.

Possible explanation

Shunting of arterial blood directly to the venous side through arteriovenous anastomosis, or to other tissues than the brain is a straightforward explanation for the discrepancy between TCD and MRI flow. For example, shunting would increase MCA flow while bypassing brain-tissue, hence leaving ftCBF unchanged. However, multiple arguments make this concept unlikely. For instance, it is currently accepted that the MCA is an end-artery, hence it contains no shunts and feeds exclusively brain-tissue. However, quantitative data on variability and functional consequences of shunts (leptomeningeal anastomoses) in humans are virtually lacking [44]. Moreover, the presence of pre-capillary arteriovenous-shunts in the brain has not been evidenced [45]. In ASL, shunting would be expected to show residual signal in venous compartments, as was observed in patients with an arterio-venous malformation [46], but not seen in healthy volunteers nor in our participants. Moreover, such assumed shunts would have to be "recruited" during exercise to accommodate an 11% increase in CBFv. Therefore, the shunting of blood flow seems an unlikely explanation and further research would be required to determine how bulk flow and tissue perfusion are related during the degree of neural recruitment involved at this type of exercise.

Correlation CBFv with rCBF

Although the interpretation of CBFv as a proxy of CBF changes in the flow territory might be difficult based on our results, TCD measurements during exercise might be considered of practical use if changes in CBFv would be directly associated with the increase in rCBF. However, no correlation between the change in CBFv and change in CBF in the precentral ROI was observed (see Figure 7.3). The present study is considered limited to assess a possible correlation between rCBF and CBFv as it employed only one intensity of exercise, and the absence of correlation should be verified with graded exercise intensities or by employing exercise with different levels of complexity. Even if such an association would be confirmed, the current observations would still introduce several conceptual difficulties.

Limitations of the present study

Some limitations pertaining to the present study must be considered. The exercise protocol in the present study was part of a larger research program, which might have influenced the present results. Prior to the handgrip exercise all subjects participated in a lower body negative pressure LBNP experiment at -50 mmHg. The LBNP exposure was performed in both the TCD and MRI session and was well tolerated by all subjects. Furthermore, minimally 15 minutes of supine rest was allowed before the start of the handgrip protocol and therefore the effect on the response to exercise was assumed to be negligible. The MRI table was modified to accommodate the LBNP box necessitating to raise subjects and head coil by 75 mm, therefore creating an offset with the magnet iso-center. This did not lead to visible decrease in image quality or artifacts; furthermore, any possible effect would impact both the CBF measurement in rest as well as the exercise-measurement, making it unlikely that the relative increase would be severely underestimated. The experiments were divided between two sessions in fixed order. Our pilot studies (unpublished data) and previous research [47,48] showed that the cardiovascular response upon exercise is highly similar when performed one week later. In the present study, comparable HR response was observed between sessions in addition to similar baseline parameters for HR, MAP and $PetCO_2$. This suggests a comparable cardiovascular response during both sessions and we therefore assume a similar cerebral hemodynamic response.

A-priori defined regions of interest (ROIs) were used to calculate the regional CBF increases. However, due to the heterogeneity of the CBF-response and the uncertainty in the exact location of the CBF response, this ROI might be sub-optimally defined. This could either result in an overestimation or an underestimation of the CBF response. An alternative approach would be the use of voxel-based statistics to define and search for clusters of significant increased CBF upon exercise. This would, however, make the ROI definition dependent on the CBF response itself and the employed threshold and it could result in large differences in ROI-volume between subjects. Therefore, the present study used an atlas to consistently define and evaluate regional CBF increase in predefined ROIs, therefore preventing a potential bias.

Visual feedback was used during the handgrip session, which could be considered a limitation of the present study. Visual stimulation is a potent stimulus and we observed a corresponding increase of 8.7% in the visual cortex ROI. The visual cortex is normally supplied by the PCA [37] and this was not investigated using TCD in the present study. The same software was used for visual feedback during both sessions, therefore a possible influence of visual stimulation on the response in the MCA territory was considered unlikely and it is assumed not to have impacted the results of this study.

CONCLUSION

During handgrip exercise ASL determined CBF does not support the claim that TCD determined changes in CBFv are a proxy for CBF changes in the relevant brain areas. The results suggest an order of magnitude difference in the measured hemodynamic response upon exercise between the two modalities. Shunting of MCA blood flow during exercise bypassing the brain tissue could be an explanation for this discrepancy. However, evidence for such a mechanism is currently lacking. Implications could be far reaching for either or both modalities, indicating the need to further explore the relation of arterial blood flow and tissue perfusion.

Acknowledgement

The authors would like to acknowledge drs. W.J. Stok for assistance in preparing and executing the experiments.

REFERENCE LIST

1. Fox PT, Raichle ME (1986) Focal physiological uncoupling of cerebral blood flow and oxidative metabolism during somatosensory stimulation in human subjects. Proceedings of the National Academy of Sciences of the United States of America 83 (4):1140-1144
2. Ide K, Horn A, Secher NH (1999) Cerebral metabolic response to submaximal exercise. J Appl Physiol 87 (5):1604-1608
3. Quistorff B, Secher NH, Van Lieshout JJ (2008) Lactate fuels the human brain during exercise. FASEB J 22 (10):3443-3449. doi:10.1096/fj.08-106104
4. Raichle ME, Grubb RL, Jr., Gado MH, Eichling JO, Ter Pogossian MM (1976) Correlation between regional cerebral blood flow and oxidative metabolism. In vivo studies in man. ArchNeurol 33 (8):523-526
5. Laughlin MH, Davis MJ, Secher NH, van Lieshout JJ, Arce-Esquivel AA, Simmons GH, Bender SB, Padilla J, Bache RJ, Merkus D, Duncker DJ (2012) Peripheral circulation. Compr Physiol 2 (1):321-447. doi:10.1002/cphy.c100048
6. Lassen NA, Ingvar DH, Skinhoj E (1978) Brain function and blood flow. Sci Am 239 (4):62-71
7. Olesen J (1971) Contralateral focal increase of cerebral blood flow in man during arm work. Brain 94 (4):635-646
8. Obrist WD, Thompson HK, Jr., Wang HS, Wilkinson WE (1975) Regional cerebral blood flow estimated by 133-xenon inhalation. Stroke 6 (3):245-256
9. Aaslid R, Markwalder TM, Nornes H (1982) Noninvasive transcranial Doppler ultrasound recording of flow velocity in basal cerebral arteries. J Neurosurg 57 (6):769-774
10. Jorgensen LG, Perko M, Hanel B, Schroeder TV, Secher NH (1992) Middle cerebral artery flow velocity and blood flow during exercise and muscle ischemia in humans. J Appl Physiol 72 (3):1123-1132
11. Jorgensen LG, Perko G, Secher NH (1992) Regional cerebral artery mean flow velocity and blood flow during dynamic exercise in humans. J Appl Physiol 73 (5):1825-1830
12. Kim YS, Seifert T, Brassard P, Rasmussen P, Vaag A, Nielsen HB, Secher NH, van Lieshout JJ (2015) Impaired cerebral blood flow and oxygenation during exercise in type 2 diabetic patients. Physiological reports 3 (6):1-13. doi:10.14814/phy2.12430
13. Hellstrom G, Fischer-Colbrie W, Wahlgren NG, Jogestrand T (1996) Carotid artery blood flow and middle cerebral artery blood flow velocity during physical exercise. J Appl Physiol 81 (1):413-418
14. Sato K, Ogoh S, Hirasawa A, Oue A, Sadamoto T (2011) The distribution of blood flow in the carotid and vertebral arteries during dynamic exercise in humans. J Physiol 589 (Pt 11):2847-2856. doi:10.1113/jphysiol.2010.204461
15. Sato K, Moriyama M, Sadamoto T (2009) Influence of central command on cerebral blood flow at the onset of exercise in women. Exp Physiol 94 (11):1139-1146
16. Friedman DB, Friberg L, Mitchell JH, Secher NH (1991) Effect of axillary blockade on regional cerebral blood flow during static handgrip. J Appl Physiol 71 (2):651-656
17. Williamson JW, McColl R, Mathews D (2003) Evidence for central command activation of the human insular cortex during exercise. J Appl Physiol 94 (5):1726-1734
18. Williamson JW, Friedman DB, Mitchell JH, Secher NH, Friberg L (1996) Mechanisms regulating regional cerebral activation during dynamic handgrip in humans. J Appl Physiol 81 (5):1884-1890
19. Williamson JW, McColl R, Mathews D, Ginsburg M, Mitchell JH (1999) Activation of the insular cortex is affected by the intensity of exercise. J Appl Physiol 87 (3):1213-1219
20. Fontes EB, Okano AH, De Guio F, Schabort EJ, Min LL, Basset FA, Stein DJ, Noakes TD (2015) Brain activity and perceived exertion during cycling exercise: an fMRI study. Br J Sports Med 49 (8):556-560. doi:10.1136/bjsports-2012-091924
21. Mehta JP, Verber MD, Wieser JA, Schmit BD, Schindler-Ivens SM (2009) A novel technique for examining human brain activity associated with pedaling using fMRI. Journal of neuroscience methods 179 (2):230-239. doi:10.1016/j.jneumeth.2009.01.029

22. King M, Rauch HG, Stein DJ, Brooks SJ (2014) The handyman's brain: a neuroimaging meta-analysis describing the similarities and differences between grip type and pattern in humans. NeuroImage 102 Pt 2:923-937. doi:10.1016/j.neuroimage.2014.05.064

23. Jørgensen LG, Perko G, Payne G, Secher NH (1993) Effect of limb anesthesia on middle cerebral response to handgrip. American journal of physiology Heart and circulatory physiology 264 (2 Pt 2):H553-H559

24. Pott F, Jensen K, Hansen H, Christensen NJ, Lassen NA, Secher NH (1996) Middle cerebral artery blood velocity and plasma catecholamines during exercise. Acta Physiol Scand 158 (4):349-356. doi:10.1046/j.1365-201X.1996.564325000.x

25. Pott F, Ray CA, Olesen HL, Ide K, Secher NH (1997) Middle cerebral artery blood velocity, arterial diameter and muscle sympathetic nerve activity during post-exercise muscle ischaemia. Acta Physiol Scand 160 (1):43-47

26. Ide K, Pott F, Van Lieshout JJ, Secher NH (1998) Middle cerebral artery blood velocity depends on cardiac output during exercise with a large muscle mass. Acta Physiol Scand 162 (1):13-20. doi:10.1046/j.1365-201X.1998.0280f.x

27. Giller CA, Giller AM, Cooper CR, Hatab MR (2000) Evaluation of the cerebral hemodynamic response to rhythmic handgrip. J Appl Physiol 88:2205-2213

28. Rasmussen P, Plomgaard P, Krogh-Madsen R, Kim YS, van Lieshout JJ, Secher NH, Quistorff B (2006) MCA Vmean and the arterial lactate-to-pyruvate ratio correlate during rhythmic handgrip. J Appl Physiol 101 (5):1406-1411. doi:10.1152/japplphysiol.00423.2006

29. Kim YS, Krogh-Madsen R, Rasmussen P, Plomgaard P, Ogoh S, Secher NH, van Lieshout JJ (2007) Effects of hyperglycemia on the cerebrovascular response to rhythmic handgrip exercise. Am J Physiol Heart Circ Physiol 293 (1):H467-473. doi:10.1152/ajpheart.00045.2007

30. Ono T, Hasegawa Y, Hori K, Nokubi T, Hamasaki T (2007) Task-induced activation and hemispheric dominance in cerebral circulation during gum chewing. J Neurol 254 (10):1427-1432. doi:10.1007/s00415-007-0570-3

31. Miyazawa T, Horiuchi M, Ichikawa D, Sato K, Tanaka N, Bailey DM, Ogoh S (2011) Kinetics of exercise-induced neural activation; interpretive dilemma of altered cerebral perfusion. Exp Physiol

32. Alsop DC, Detre JA, Golay X, Gunther M, Hendrikse J, Hernandez-Garcia L, Lu H, MacIntosh BJ, Parkes LM, Smits M, van Osch MJ, Wang DJ, Wong EC, Zaharchuk G (2015) Recommended implementation of arterial spin-labeled perfusion MRI for clinical applications: A consensus of the ISMRM perfusion study group and the European consortium for ASL in dementia. Magnetic resonance in medicine : official journal of the Society of Magnetic Resonance in Medicine / Society of Magnetic Resonance in Medicine 73 (1):102-116. doi:10.1002/mrm.25197

33. Ghariq E, Chappell MA, Schmid S, Teeuwisse WM, van Osch MJ (2014) Effects of background suppression on the sensitivity of dual-echo arterial spin labeling MRI for BOLD and CBF signal changes. NeuroImage 103:316-322. doi:10.1016/j.neuroimage.2014.09.051

34. Ye FQ, Frank JA, Weinberger DR, McLaughlin AC (2000) Noise reduction in 3D perfusion imaging by attenuating the static signal in arterial spin tagging (ASSIST). Magnetic resonance in medicine : official journal of the Society of Magnetic Resonance in Medicine / Society of Magnetic Resonance in Medicine 44 (1):92-100

35. Wang Z, Aguirre GK, Rao H, Wang J, Fernandez-Seara MA, Childress AR, Detre JA (2008) Empirical optimization of ASL data analysis using an ASL data processing toolbox: ASLtbx. Magnetic resonance imaging 26 (2):261-269. doi:10.1016/j.mri.2007.07.003

36. Tzourio-Mazoyer N, Landeau B, Papathanassiou D, Crivello F, Etard O, Delcroix N, Mazoyer B, Joliot M (2002) Automated anatomical labeling of activations in SPM using a macroscopic anatomical parcellation of the MNI MRI single-subject brain. NeuroImage 15 (1):273-289. doi:10.1006/nimg.2001.0978

37. Tatu L, Moulin T, Bogousslavsky J, Duvernoy H (1998) Arterial territories of the human brain: cerebral hemispheres. Neurology 50 (6):1699-1708

38. Kontos HA (1989) Validity of cerebral arterial blood flow calculations from velocity measurements. Stroke 20 (1):1-3

39. Gevers S, Nederveen AJ, Fijnvandraat K, van den Berg SM, van OP, Heijtel DF, Heijboer H, Nederkoorn PJ, Engelen M, van Osch MJ, Majoie CB (2012) Arterial spin labeling measurement of cerebral perfusion in children with sickle cell disease. J Magn Reson Imaging 35 (4):779-787. doi:10.1002/jmri.23505 [doi]

40. Dai W, Garcia D, de BC, Alsop DC (2008) Continuous flow-driven inversion for arterial spin labeling using pulsed radio frequency and gradient fields. Magnetic resonance in medicine 60 (6):1488-1497

41. Petersen ET, Zimine I, Ho YC, Golay X (2006) Non-invasive measurement of perfusion: a critical review of arterial spin labelling techniques. Br J Radiol 79 (944):688-701. doi:10.1259/bjr/67705974

42. Verbree J, Bronzwaer A, van Buchem MA, Daemen M, van Lieshout JJ, van Osch M (2016) Middle cerebral artery diameter changes during rhythmic handgrip exercise in humans. J Cereb Blood Flow Metab. doi:10.1177/0271678X16679419

43. Hellström G, Fischer-Colbrie W, Wahlgren NG, Jøgestrand T (1996) Carotid artery blood flow and middle cerebral artery blood flow velocity during physical exercise. J Appl Physiol 81 (1):413-418

44. Brozici M, van der Zwan A, Hillen B (2003) Anatomy and functionality of leptomeningeal anastomoses: a review. Stroke 34 (11):2750-2762. doi:10.1161/01.str.0000095791.85737.65

45. Duvernoy HM, Delon S, Vannson JL (1981) Cortical blood vessels of the human brain. Brain Res Bull 7 (5):519-579

46. Le TT, Fischbein NJ, Andre JB, Wijman C, Rosenberg J, Zaharchuk G (2012) Identification of venous signal on arterial spin labeling improves diagnosis of dural arteriovenous fistulas and small arteriovenous malformations. Am J Neuroradiol 33 (1):61-68. doi:10.3174/ajnr.A2761

47. Sinoway L, Shenberger J, Leaman G, Zelis R, Gray K, Baily R, Leuenberger U (1996) Forearm training attenuates sympathetic responses to prolonged rhythmic forearm exercise. J Appl Physiol 81 (4):1778-1784

48. Lopez MG, Silva BM, Joyner MJ, Casey DP (2012) Ischemic exercise hyperemia in the human forearm: reproducibility and roles of adenosine and nitric oxide. Eur J Appl Physiol 112 (6):2065-2072. doi:10.1007/s00421-011-2035-8